European Journal of Medicinal Chemistry 161 (2019) 533–542

Contents lists available at ScienceDirect

European Journal of Medicinal Chemistry

journal homepage: http://www.elsevier.com/locate/ejmech

Research paper

# Investigation of the molecular characteristics of bisindole inhibitors as HIV-1 glycoprotein-41 fusion inhibitors

Guangyan Zhou [a], Shidong Chu [a], Ariana Nemati [a], Chunsheng Huang [c], Beth A. Snyder [c], Roger G. Ptak [c], Miriam Gochin [a, b, *]

[a] Department of Basic Sciences, Touro University-California, Vallejo, CA, 94592, USA
[b] Department of Pharmaceutical Chemistry, University of California San Francisco, CA, 94143, USA
[c] Southern Research Institute, 431 Aviation Way, Frederick, MD, 21701, USA

ARTICLE INFO

*Article history:*
Received 22 August 2018
Received in revised form
18 October 2018
Accepted 19 October 2018
Available online 23 October 2018

*Keywords:*
HIV-gp41
Fusion inhibitor
Bisindole
Suzuki coupling
Sub-μM activity

ABSTRACT

In previous work, we described 6-6'-bisindole compounds targeting a hydrophobic pocket on the N-heptad repeat region of viral glycoprotein-41 as effective inhibitors of HIV-1 fusion. Two promising compounds with sub-micromolar $IC_{50}$'s contained a benzoic acid group and a benzoic acid ester attached at the two indole nitrogens. Here we have conducted a thorough structure-activity relationship (SAR) study evaluating the contribution of each of the ring systems and various substituents to compound potency. Hydrophobicity, polarity and charge were varied to produce 35 new compounds that were evaluated in binding, cell-cell fusion and viral infectivity assays. We found that (a) activity based solely on increasing hydrophobic content plateaued at ~ 200 nM; (b) the bisindole scaffold surpassed other heterocyclic ring systems in efficacy; (c) a polar interaction possibly involving Gln575 in the pocket could supplant less specific hydrophobic interactions; and (d) the benzoic acid ester moiety did not appear to form specific contacts with the pocket. The importance of this hydrophobic group to compound potency suggests a mechanism whereby it might interact with a tertiary component during fusion, such as membrane. A promising small molecule **10b** with sub-μM activity was discovered with molecular weight <500 da and reduced logP compared to earlier compounds. The work provides insight into requirements for small molecule inhibition of HIV-1 fusion.



## 1. Introduction

Previous studies by our lab and others on small molecule inhibition of HIV-1 fusion have revealed the importance of hydrophobic groups and negative charge for measurable bioactivity [1–4]. Inhibitors bind to a hydrophobic cavity within the ectodomain of transmembrane glycoprotein gp41 that is exposed during fusion [5], and potency is generally correlated to pocket binding affinity [2,6]. The cavity is defined by N-heptad repeat (NHR) residues 565–579 on two chains of the gp41 homotrimer (HXB2 numbering). It is lined by several non-polar branched chain amino acids and a nearby tryptophan, but also includes polar residues Thr and Gln, as well as positively charged Lys and Arg residues that likely lead to the requirement for negative charge on pocket-binding inhibitors. These inhibitors block the interaction between two protein domains of gp41, the NHR trimer containing the hydrophobic pocket and gp41 C-heptad repeat (CHR) helices that bind in the pocket following a gp41 conformational change during fusion [7]. The specific pocket binding domain of the CHR is Trp-x-x-Trp-Asp-x-x-Ile where Trp and Ile residues intercalate within the pocket and Asp forms a salt bridge with the pocket Lys [8].

Studies of protein-protein interaction inhibitors (PPI) have generally revealed that they are more hydrophobic, more aromatic and larger than drugs targeting enzymes [9–11]. Analysis of recent small molecule PPI modulators currently in the clinic revealed a broad range of molecular sizes and complexity, particularly with a logP range of 1.6–10.5 [12]. Efficiency of binding to the hydrophobic patch at the core of the protein –protein interaction surface was cited [11] as a key determinant of potency. In previous studies, we identified a promising scaffold containing two 6-6′ connected indole rings B and C supporting substituted benzyl rings A and D at positions 1 or 3 on the indole rings (Fig. 1) [2,6,13]. A structure-

* Corresponding author. Touro University - California, 1310 Club Drive, Mare Island, Vallejo, CA, 94592, USA.
*E-mail address:* miriam.gochin@tu.edu (M. Gochin).

https://doi.org/10.1016/j.ejmech.2018.10.048
0223-5234/

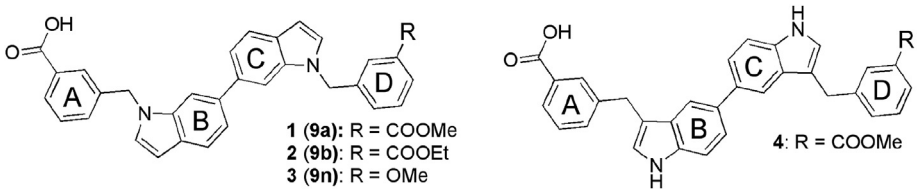


**Fig. 1.** Bisindole scaffold structure. Compounds **1**–**4** are shown, and their equivalents in the current study.

activity relationship (SAR) study upheld the contention that hydrophobicity played an essential role in potency, as did having a negative charge on the ligand. The following key features were observed: 1) A free carboxylic acid on ring A was indispensable for activity. 2) Ring D conferred an order of magnitude improvement in antiviral potency compared to three ring (A-B-C) compounds, with the *m*-benzoic acid ester providing optimal performance (compounds **1**, **2** Fig. 1, $IC_{50} = 0.3–0.4\ \mu M$), and the *m*-methoxy group also being favorable (compound **3**, Fig. 1, $IC_{50} = 0.8\ \mu M$). 3) Indole 1, 1′ substitution was preferred over 3, 3′ substitution (compound **4**, Fig. 1, $IC_{50} = 5.0\ \mu M$), as was indole over benzimidazole [2], suggesting that the hydrophobic surface presented by the outer vertices of rings B and C was critical for activity. 3) Variation of nonpolar substituents on ring D had a mild effect on potency (~2-fold), while a charged substituent on ring D such as carboxylic acid yielded two orders of magnitude reduced antiviral potency, even though binding affinity for the hydrophobic pocket (HP) did not diminish. The in vivo effect suggested that membrane could play a role in bioactivity. The deleterious effect caused by adding more than one negative charge might be attributed to polar head groups of phospholipids repelling a negatively charged ligand. In this sense, the protein-protein domain interaction may be complicated by proximity of the pocket to membrane. And, while increasing hydrophobicity could increase interactions within the pocket, it might also render the molecules less soluble and potentially nonspecific. Thus a delicate balance of hydrophobicity and charge is required to maximize the inhibitory potential of the ligands.

Here we set out to explore this balance by making additional changes to the scaffold to increase or decrease hydrophobic contact points, or substitute polar moieties in order to sustain or increase solubility and potentially introduce hydrogen bonds. Modification strategies were based in part on docking studies predicting a narrow S-shaped structure for the compounds, conforming to the shape of the hydrophobic groove [2]. Fig. 2 shows the array of polar and nonpolar residues lining the pocket with an overlay of several docked structures described in the current study. We note that the modeling is limited by a lack of complete knowledge of HP structure [14]. We examined $^{19}F$ substitution on different rings, made additional substitutions on ring D, replaced indoles B and/or C with chemically similar alternatives, and varied the linkage between rings C and D. Overwhelmingly the results confirmed the bisindole scaffold as the optimal choice, and showed that simply increasing hydrophobic interactions did not yield a significant increase in potency. The SAR indicated that indole B interactions with pocket residues contributed more than those of indole C, suggesting that B is buried more deeply within the pocket. The methylene linker between ring C and D could be substituted with a sulfoxy or carbonyl group, suggesting that polar contacts could occur with pocket residues. A three-ring compound **10b** was identified as the first example of a sub-μM inhibitor with a molecular weight <500 da.

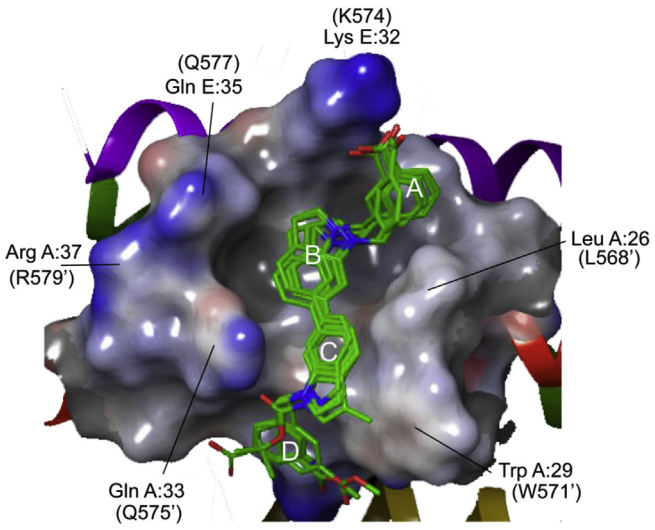


**Fig. 2.** Predicted conformation of several ligands in the current study in the hydrophobic pocket of PDB structure *2xra*. Residue numbers in the construct are shown together with their corresponding HXB2 Env numbers in brackets. The two chains making up the binding site are distinguished by E and A in the *2xra* construct or by using a prime to mark the second chain in HXB2 numbering. Ligands shown are **9g**, **10b**, **9c**, **15b**, **9j**, **11g**.

## 2. Results

### 2.1. Effect of fluorine substitution

Fluorine is a small atom with high electronegativity, slightly larger than a hydrogen atom. It has been introduced into medicinal candidates not only to improve metabolic stability but also binding affinity to the target protein. Fluorine substitution could lead to a slightly increased nonspecific lipophilicity [15,16]. The effect of fluorine substitution on the intrinsic potency of the bisindole compounds is shown in Table 1. Introduction of fluorine on rings A, C and/or D reduced potency by up to 10-fold, compared to the corresponding hydrogen counterparts. We observed two cases in which a single fluorine substitution at any position had a significant deleterious effect, while a subsequent second fluorine substituent had little additional effect on potency. For example, in order of potency, **11a** > **11h** ≈ **11i**; **9a** ≫ **9o** ≈ **9p**. However, a more varied effect was observed for other compounds. A single fluorine at the 5 position of indole C or at the meta position of ring D on **9a** left activity slightly lower but still at sub-μM levels (**15d**, **9d**). The same 5-F-indole substitution on compound **3**, however, led to a 10-fold reduction in potency (**9q**). $K_I$ for HP binding was correlated to observed antiviral activity for the compounds in Table 1, ($R^2 = 0.80$ (CCF); $R^2 = 0.58$ (VCF)). The drop in potency upon fluorine substitution may be a result of decreased solubility associated with increased hydrophobicity. Among the five variants of **9a** in Table 1, a strong correlation ($R^2 = 0.93$) was observed between increase in logP and loss of potency in cell-based assays. The effect was more pronounced when starting with compounds having a higher logP (**9a** and **9n** vs. **11a**). Therefore we observed that fluorination did not improve potency in the case where compounds were already highly hydrophobic.

**Table 1**
Testing fluorine substitutions on bisindole compounds.

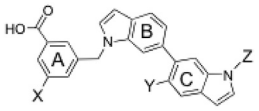


| | X | Y | Z | MWt | logP[a] | log S[b] | $K_I$ (HP)[c] | $IC_{50}$ CCF[c] | $IC_{50}$ VCF Ba-L[c] | $IC_{50}$ VCF IIIB[c] | $CC_{50}$[c] |
|---|---|---|---|---|---|---|---|---|---|---|---|
| **11i** | F | F | $CH_3$ | 416.4 | 6.84 | −8.03 | 2 | 2 | 9.7 | 7.8 | >20 |
| **11h** | F | H | $CH_3$ | 398.4 | 6.61 | −7.63 | 3 | 3.6 | 8.2 | 9.1 | >20 |
| **11a**[d] | H | H | $CH_3$ | 380.4 | 6.42 | −7.42 | 1.4 | 1.3 | 4.5 | 4.3 | >50 |
| **15d** | H | F | 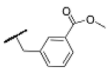 | 532.6 | 7.88 | −9.84 | 0.7 | 0.4 | 0.5 | 0.4 | >20 |
| **9a**[d] | H | H | 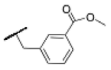 | 514.6 | 7.88 | −10.12 | 0.6 | 0.2 | 0.4 | 0.3 | >20 |
| **9d** | H | H | 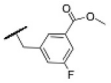 | 532.6 | 7.51 | −8.77 | 1 | 0.8 | 0.4 | 0.5 | >20 |
| **9o** | H | H | 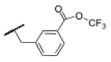 | 540.5 | 9.10 | −10.13 | 2.3 | 1.4 | 1.4 | 1.5 | >20 |
| **9p** | F | H | 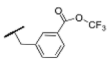 | 558.5 | 9.62 | −11.34 | 1.7 | 2.1 | 1.4 | 2.0 | >20 |
| **9q** | H | F |  | 504.6 | 8.23 | −9.30 | 5 | 3.5 | 9.4 | 7.0 | >20 |
| **9n**[d] | H | H |  | 486.6 | 8.11 | −9.20 | 1 | 0.8 | 0.8 | 0.9 | >25 |

[a] Calculated water-octanol partition coefficient.
[b] Calculated solubility.
[c] All values in μM.
[d] Previously published in Ref. [2].

### 2.2. Examination of substituents at group D

Previous observation of the important contribution of benzyl ring D to antiviral potency, as well as the loss of potency associated with addition of a negatively charged substituent on D spurred us to consider additional substituent changes at this location. The best performing compounds contained a carboxylic acid ester substituent, although this position is exposed to solvent in predicted binding orientations (Fig. 2). We examined additional molecules to confirm this effect. Table 2 shows the results. The *t*-Bu ester on ring D (compound **9c**) has increased hydrophobicity compared to **9a** (methyl ester) and **9b** (ethyl ester) and showed marginally improved antiviral activity ($IC_{50} = 0.2$ μM). Increasing hydrophobic bulk by adding a second *m*'-carbomethoxy group to form **9e** slightly reduced antiviral activity ($IC_{50}^{VCF} = 0.6$ μM), as did adding a *m*'-F substituent in **9d**, ($IC_{50}^{VCF} = 0.5$ μM). Adding the *m*-carbomethoxy group to a *p*-OMe substituted ring D had an even more pronounced negative effect (**9f**, $IC_{50}^{VCF} = 3–4$ μM). Thus added hydrophobic bulk at ring D was not tolerated. We previously observed that a negatively charged *m*-carboxylate was highly deleterious (compound **9g**, $IC_{50}^{VCF} = 60$ μM) [2], and confirmed this effect with a new compound having both a *m*-carboxylate and *m*'-methoxy group (compound **9h**). This compound had 15-fold lower activity against CCF compared to **9n** and no measurable antiviral activity up to 20 μM. These two compounds both exhibited sub-μM binding affinity to the HP, similar to that of compounds **9a**, **9b** and **9n**.

We further explored the polarity at ring D with a nitro group and a series of amine substitutions. Compounds **9i**, **9j**, **9k**, **9l** were much more active than **9g**. Three of them had lower activity ($IC_{50} = 1.2–4.7$ μM) than **9a**. One of them, **9l**, had sub-μM activity ($IC_{50} = 0.5$ μM), marginally lower than that of **9a**. Switching D to a saturated six-membered piperidine ring did not significantly impact activity (compound **9r**, $IC_{50} = 0.6$ μM). The sub-μM activity of **9l** and **9r** may in part be attributed to the hydrophobic *t*-Bu carboxylate ester associated with added benefit in **9c**.

For the compounds in Table 2, the $K_I$ for solution binding did not correlate well to $IC_{50}$, driven by the discrepancy observed for the −COOH − substituted and to some extent the −NH- substituted compounds Therefore the binding assay did not fully recapitulate the *in situ* mechanism, implying that other biological components may be involved. It is possible that polarity due to an N−H or C═O group, together with hydrophobic esterification, supports insertion of ring D into anionic phospholipid membrane or an anionic lipophilic protein domain. This would explain the detrimental effect of a negatively charged substituent on D and the failure of the solution binding experiment to correctly predict activity of **9g** and **9h**.

### 2.3. Adjustment of the linker between groups C and D

Due to the proximity of Gln 575′ to the predicted pose of the compounds, the potential for a polar interaction was tested by converting the methylene of the benzyl group of D into sulfonyl or carbonyl. In the −CO- containing compound, the phenyl group was replaced entirely by a *t*-Bu ester, which proved to be successful as a

**Table 2**
Testing substituents at ring D.

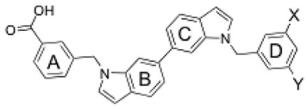


| | X | Y | MWt | logP[a] | log S[b] | $K_I$ (HP)[c] | $IC_{50}$ CCF[c] | $IC_{50}$ VCF Ba-L[c] | $IC_{50}$ VCF IIIB[c] | $CC_{50}$[c] |
|---|---|---|---|---|---|---|---|---|---|---|
| **9a** [d] | $-COOCH_3$ | -H | 514.6 | 7.88 | −10.12 | 0.6 | 0.2 | 0.4 | 0.3 | >20 |
| **9b** [d] | $-COOCH_2CH_3$ | -H | 528.6 | 8.13 | −9.90 | 1.0 | 0.7 | 0.3 | 0.5 | >40 |
| **9c** | $-COOC(CH_3)_3$ | -H | 556.7 | 8.36 | −9.21 | 0.3 | 0.2 | 0.2 | 0.2 | >10 |
| **9d** | $-COOCH_3$ | -F | 532.6 | 7.51 | −8.77 | 1.0 | 0.8 | 0.4 | 0.5 | >20 |
| **9e** | $-COOCH_3$ | $-COOCH_3$ | 572.6 | 7.45 | −10.11 | 1.0 | 0.2 | 0.6 | 0.6 | >20 |
| **9f** | $-COOCH_3$ | $-OCH_3$ (p)[e] | 544.6 | 7.82 | −9.27 | 0.4 | 2 | 4.2 | 3.1 | ~25 |
| **9g** [d] | -COOH | -H | 500.6 | 7.40 | −9.14 | 0.6 | 12 | 58 | 67 | >100 |
| **9h** | -COOH | $-COOCH_3$ | 548.6 | 7.44 | −9.09 | 0.8 | 8 | >20 | >20 | >20 |
| **9i** | $-NO_2$ | -H | 501.5 | 7.33 | −9.22 | 2.7 | 2 | 2.8 | 3.4 | >20 |
| **9j** | $-NH_2$ (p)[a] | -H | 471.6 | 7.11 | −8.81 | 3.1 | 3 | 1.1 | 1.3 | >20 |
| **9k** | $-NH-COCH_3$ | -H | 513.6 | 7.46 | −9.45 | 0.9 | 1 | 4.7 | 4.5 | >20 |
| **9l** | $-NH-COOC(CH_3)_3$ | -H | 571.7 | 8.53 | −10.79 | 1.5 | 2 | 0.4 | 0.5 | >20 |
| **9r** | 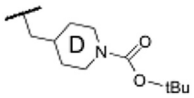 | | 563.7 | 8.24 | −7.79 | 1.2 | 1.2 | 0.6 | 0.6 | >20 |



[a] Calculated water-octanol partition coefficient.
[b] Calculated solubility.
[c] All values in μM.
[d] Previously published in Ref. [2].
[e] Para substituted.

substituent on the ring. The results are shown in Table 3. $-SO_2-$ substitution for $-CH_2-$ by attachment of a *p*-methylphenylsulfonyl group as ring D led to compound **10a** with $IC_{50} = 0.9$ μM, the same potency as that of **9m**, containing a *p*-trifluoromethyl benzyl group as ring D. Although fluorine substitution is likely to have reduced the bioactivity of **9m** compared to a protonated counterpart (not measured), based on results shown in Table 1, the sub-μM potency of **10a** is in line with that of other 4-ring compounds. The relative reduction in logP of at least 1.6 units, meanwhile, suggests that a polar interaction involving the $-SO_2-$ moiety is substituting for hydrophobic contacts. −CO- as the linker, in the form of the Boc group, yielded significant enhancement of potency compared to previous compounds lacking a benzyl group at D (ref [2] and Table 4), with **10b** displaying 0.9–1.0 μM antiviral activity. Both molecular weight and logP are substantially lower than for compounds with ≤1.0 μM activity discussed in Tables 1 and 2.

Although limited in scope, the results here suggest that a polar interaction, likely with a Gln in the pocket, replaced previous hydrophobic interactions conferred by the $CH_2$ linker. Virtual docking (Glide docking, Schrodinger, LLC, New York, NY, 2018) revealed a common binding pose, adopted by most ligands, that is shown in Fig. 2. Fig. 3 shows the ligand interaction diagram for 10b. The core of the inhibitor fit into a hydrophobic channel defined by Leu568' (Leu A:26), Val570 (Val E:28), Trp571' (Trp A:29) and Ile573 (Ile E:31). Two putative H-bonds were present. The first, between the carboxylate on ring A and Lys 574 (Lys E:32) was commonly observed for all docked compounds in this study. For 10a and 10b, an additional hydrogen bond formed between the sulfonyl or carbonyl group and Gln 575' (Gln A:33). The -O-tBu group of 10b is solvent exposed in this model, although it is clearly important since saponification reduced activity by a factor of 5 (data not shown). Additionally, the $K_I$ of 10b did not accurately reflect its bioactivity, implying that the *t*-Bu group may be involved in interactions other than pocket binding. 10a docked in an identical binding mode to 10b with the added potential of ring stacking between ring D and Trp 571′. The lower molecular weight and/or 20–30% reduction in logP of 10a and 10b compared to 9 m and other 4-ring compounds in Table 2 indicated an improvement in drug-like characteristics

**Table 3**
Testing added polarity in the C-D connector.

| | Group D[d] | MWt | logP[a] | log S[b] | $K_I$ (HP)[c] | $IC_{50}$ CCF[c] | $IC_{50}$ VCF Ba-L[c] | $IC_{50}$ VCF IIIB[c] | $CC_{50}$[c] |
|---|---|---|---|---|---|---|---|---|---|
| **10a** |  | 520.6 | 6.25 | −7.99 | 1.2 | 1.3 | 0.8 | 0.9 | >50 |
| **9m**[a,e] | 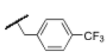 | 524.5 | 8.98 | −9.69 | 1 | 2 | 0.9 | 1.0 | >50 |
| **10b** |  | 466.5 | 6.81 | −8.72 | 1.9 | 0.8 | 0.9 | 1.0 | >20 |



[a] Calculated water-octanol partition coefficient.
[b] Calculated solubility.
[c] All values in μM.
[d] Groups A, B, C and linker position as in Table 2.
[e] Previously published in Ref. [2].

**Table 4**
Testing modifications at rings B, C.[a]

| | Group B | Group C | Group D | MWt | logP[c] | log S[d] | $K_I$ (HP)[e] | $IC_{50}$ CCF[e] | $IC_{50}$ VCF Ba-L[e] | $IC_{50}$ VCF IIIB[e] | $CC_{50}$[e] |
|---|---|---|---|---|---|---|---|---|---|---|---|
| **11a** [f] | Indole | Indole | $CH_3$ | 380.4 | 6.42 | −7.42 | 1.4 | 1.3 | 4.5 | 4.3 | >50 |
| **11b** [g] | Indazole | Indole | $CH_3$ | 399.4 | 5.97 | −7.29 | 2.1 | 4.6 | >20 | >20 | >20 |
| **11c1** [g] | Indole | Indazole | 1-$CH_3$ | 399.4 | 5.93 | −7.31 | 2.5 | 7 | 10.1 | 11.3 | >20 |
| **11c2** [g] | Indole | Indazole | 2-$CH_3$ | 399.4 | 5.69 | −6.84 | 6.4 | 28 | 14 | >20 | >20 |
| **11e** [g] | Indazole | Indazole | 1-$CH_3$ | 400.4 | 5.41 | −7.10 | 19 | >25 | >20 | >20 | ~200 |
| **11f** | Indoline | indole | $CH_3$ | 382.5 | 3.58 | −5.74 | 10 | >10 | >25 | >25 | >50 |
| **9n** [f] | Indole | Indole |  | 486.6 | 8.11 | −9.20 | 1 | 0.8 | 0.8 | 0.9 | >25 |
| **9s** | 3-Me-indole | Indole |  | 500.6 | 8.31 | −8.50 | 1.2 | 4 | 10.5 | 12.9 | ~70 |
| **15e** | indole | Indoline |  | 488.6 | 5.40 | −8.65 | 3.6 | 1 | 1.9 | 2.4 | >25 |
| **15f** | Indazole[b] | indole |  | 487.6 | 7.53 | −9.13 | 1.0 | n.d. | 5.8 | 5.5 | >20 |
| **18d** | indole | *m*-aniline |  , H | 462.5 | 7.20 | −8.47 | 1.5 | >10 | >20 | >20 | >10 |
| **18a** | indole | *m*-aniline |  , $CH_3$ | 476.6 | 7.78 | −8.44 | 0.8 | 1.6 | 1.6 | 1.2 | >20 |
| **18c** | indole | *m*-aniline |  | 562.7 | 8.60 | −10.56 | 0.45 | 4.2 | 5.5 | 4.2 | >10 |
| **11d** | Indole | Indoline |  | 468.6 | 6.88 | −9.00 | 0.9 | 2.9 | 2.3 | 2.8 | >25 |
| **11g** | indole | 3-Me-indole |  | 480.6 | 7.24 | −9.60 | 4.7 | 2.6 | 1.2 | 1.7 | >20 |
| **18b** | indole | *m*-aniline |  , $CH_3$ | 456.5 | 6.95 | −8.95 | 1.6 | 5.9 | 15.6 | 11.3 | >20 |
| **15b** | indole | Indazole | 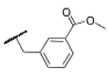 | 515.6 | 7.20 | −9.43 | 1.0 | 0.3 | 1.4 | 1.4 | >50 |
| **15c** | indazole | Indole | 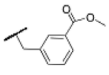 | 515.6 | 6.96 | −8.82 | 3.2 | 2.8 | 3.1 | 2.5 | >20 |

[a] Group A is connected at N1 of group B except.
[b] Connected at N2 of indazole; group D is connected at N1 (indole, indazole, indoline) or N (aniline) of group C.
[c] Calculated water-octanol partition coefficient.
[d] Calculated solubility.
[e] All values in μM.
[f] Previously published in Ref. [2].
[g] *m*-F on ring A.

while activity was retained.

### 2.4. Examination of the molecular core

The 6-6′ bisindole scaffold influences the shape of the inhibitors, and is predicted to contribute significant interactions with surrounding amino acids when buried in the hydrophobic pocket. To further understand the importance of the scaffold, alternative heterocyclic rings were substituted for indoles to test specific interactions. Thus indole groups were exchanged (Fig. 4) for indoline, 3-methyl-indole, aniline or indazole. In previous studies, we determined that adding a polar nitrogen atom at vertex 3 (by benzimidazole substitution) caused a 50-fold loss in potency [2]. Saturation of the 2–3 double bond in indoline is accompanied by loss of full planarity. Adding a methyl group at position 3 increases hydrophobic content and bulk, while an N-methyl substituted aniline “removes” vertex 3 completely, compared to an indole. Without the methyl group on the aniline nitrogen, vertices 2 and 3 are both absent. We also tested indazole with nitrogen at position 2 as a potential substitute for indole, allowing for increased inhibitor polarity while perhaps not having the negative effect of a benzimidazole. Indazole and indoline groups are regularly used in biological or pharmaceutical research [17–19]. The SAR, shown in Table 4, was conducted concurrently with variation in group D and we therefore identified four reference compounds, 9a, 9n, 10b, 11a to which the non-bisindole containing compounds could be compared. They have group D = *m*-methylbenzoate, *m*-methoxybenzyl, Boc and methyl, respectively. The results of Table 4 are summarized in Table 5 as an activity score relative to the reference compounds. Substituting any of the heterocyclic variants for indole at position B resulted in at least a six-fold loss of potency. For example, substituting indole with indazole or 3-methylindole at position B caused a 10-fold reduction in activity in either case (15c vs 9a, 9s vs. 9n). 11f, with an indoline at position B, had no

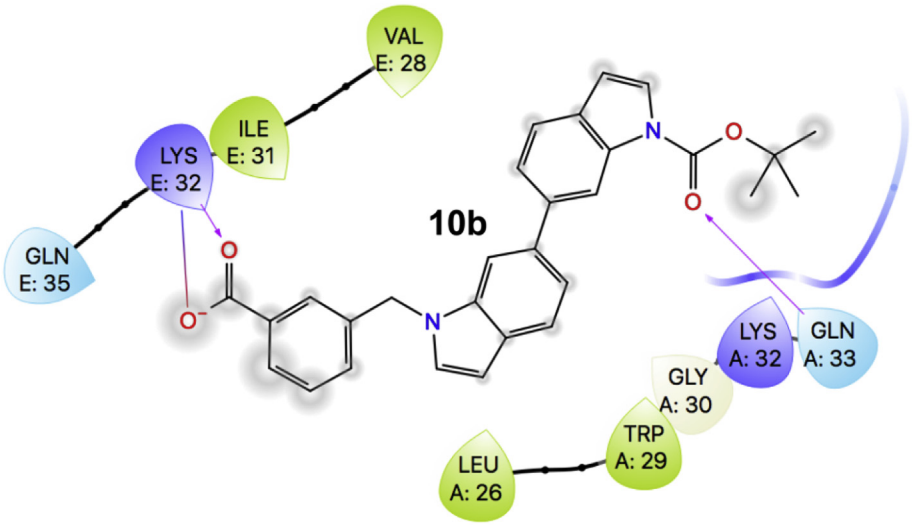


**Fig. 3.** Interaction diagram for virtually docked ligand 10b in the pocket of *2xra* (Glide docking). Negative and hydrophobic residues surrounding the ligand are shown in purple and green respectively, while polar residues are shown in blue. Hydrogen bonds to carbonyl groups are shown as magenta colored arrows, and an additional salt bridge interaction with the carboxylate group is represented by a line. Solvent exposure is indicated by grey circles, with the size reflecting the degree to which each vertex is exposed. Residue numbers shown are those for the *2xra* construct, with residues 26–35 corresponding to HXB2 residues 568–577 (see also Fig. 2). (For interpretation of the references to color in this figure legend, the reader is referred to the Web version of this article.)

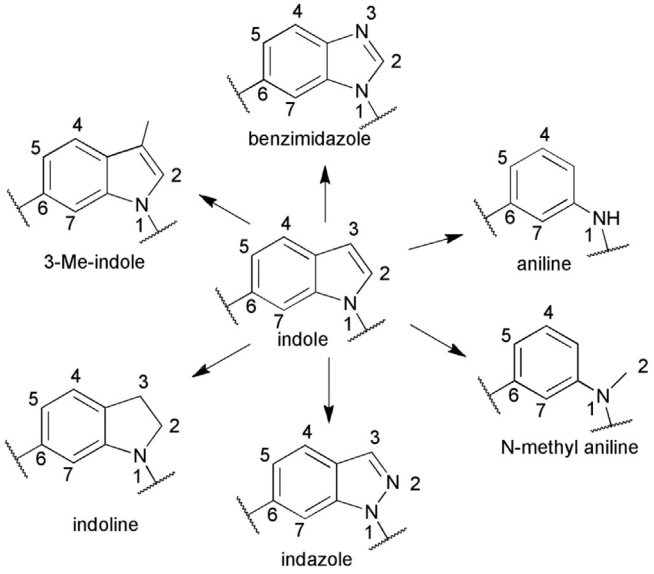


**Fig. 4.** Substitutions of alternative single ring or fused ring structures for indole at the core of the molecular scaffold, showing the changes in vertex character at the equivalent of indole positions 2 and 3.

observable activity, compared to 11a which had $IC_{50} = 4\,\mu M$. Interestingly, the calculated logP for 11f is relatively low (3.58), which could be a factor in its lack of activity, and might suggest a lower limit of logP for successful intervention in the HP. Changes of ring C had a more moderate effect on bioactivity, typically a factor of 2–3, except for substitution with an aniline which had varied effects. Changing hydrophobicity at the 3-position of indole C (with an indoline in 11d or with 3-methylindole in 11g) was detrimental, but removing this vertex in 18b by substituting an N-methylated aniline or removing both vertices 2 and 3 in 18d also had a negative effect. Substitution with aniline, in addition to affecting local interactions, increases molecular flexibility because of free rotation of the carbon-nitrogen bond. This can potentially alter the interactions of group D and introduce an entropic penalty upon binding, making it difficult to fully interpret observed changes in activity. Nevertheless it is apparent that aniline-containing compounds performed poorly. As an example, the potency of 10b containing an indole at C and Boc group replacing D was unique, since the benefits of substitution of Boc for benzyl did not extend to a compound with aniline at the C position, i.e. 18b was much worse than 18a (Table 4). Increased bulk of the substituents at the aniline nitrogen was also tested in series 18d, 18a and 18c, with an improvement in $K_I$ for HP binding and mixed results in bioactivity. Some of this could be due to decreased solubility associated with the increase in hydrophobicity, but as observed for compounds in Table 2 we again see that increasing bulk at this end of the molecule was counterproductive.

Unlike indole or indoline, the indazole group can be linked to group D and/or A at N2 as well as N1. N2-linked isomers (11c2 and 15f) proved to have lower activity compared to N1-linked counterparts and were not explored further.

In summary, an indole at position B seemed to be essential for good bioactivity. Additionally, none of the tested compounds was consistently better than with an indole at position C. These results speak strongly to the need for the bisindole shape and likely tight fit within the groove of the HP. They also suggest that indole B is more deeply buried in the pocket, in agreement with the predicted binding pose (Fig. 2).

## 3. Discussion

In this study, we designed, synthesized and tested a series of compounds based on a bisindole scaffold as entry inhibitors against HIV-1 gp41. The bisindole scaffold consisted of 4 rings A-B-C-D attached linearly, with A = benzoic acid, B and C = indole and D = a substituted benzyl group. Variations included substituting B and C indoles with alternative fused ring or single ring structures, examining substitutions on or for ring D, and replacing hydrogen with fluorine at different positions. The following findings were observed:

*Activity reached a plateau with increasing hydrophobicity* Several of the new compounds had sub-μM activity against viral infectivity and cell-cell fusion, and the most active compound 9c exhibited

**Table 5**
Exploring the character of B – C moieties.

| Group B | Group C | Fold increase in $IC_{50}^{VCF}$[a] | Example compounds |
|---|---|---|---|
| indole | indole | 1 | 9a, 9n, 10b, 11a[b] |
| indole | indoline | 2 | 15e vs. 9n; 11d vs. 10b |
| indole | 3-Me-indole | 2 | 11g vs 10b |
| indole | indazole | 2 | 15b vs 9a; 11c vs 11a |
| indole | aniline | 2–20 | 18b vs. 10b (15); 18d vs. 10b (>20); 18a vs. 9n (2) |
| indazole | indole | ≥6 | 11b vs. 11a; 15c.vs.9a |
| 3-Me-indole | indole | 10 | 9s vs. 9n |
| indoline | indole | >6 | 11f vs 11a |
| indazole | indazole | >5 | 11e vs. 11a |

[a] Inhibition of virus – cell infectivity.
[b] Reference compounds defined by substituent D, for comparison with non - bisindole variants.

binding affinity $K_I = 0.3\,\mu M$ and $IC_{50}^{VCF} = 0.2\,\mu M$ against fusion. However, this compound has a high logP (8.36) and low predicted solubility (logS = −9.21), beyond the range of drug-like characteristics and possibly incurring non-specific hydrophobic interactions and/or toxicity at high concentrations [20]. Studies of fluorinated derivatives revealed that increasing logP was detrimental to activity, suggesting an upper limit beyond which bioavailability is impacted for this class of compounds. Increased hydrophobicity could mask the potency of the compounds in cell-based assays because of the reduced solubility.

*6-6′ bisindole was the preferred scaffold* By substituting various alternative fused ring or single ring moieties for indole, we found that the 6-6'-bisindole remained the preferred scaffold. It is likely that this structure conforms well to the gp41 pocket shape as we have previously surmised [2]. The group B indole was particularly important and docking studies show it making 14 close contacts (≤4 Å) with atoms on Ile 573, Lys 574 and Gln 577, while indole C made 6 close contacts with atoms on Leu 568′ and Trp 571'.

*Position D may contribute a ternary interaction with lipids* We discovered that the exact nature of substitutions at position D did not significantly impact activity, other than the requirement that they not involve negative charge or significantly added bulk. Yet ring D or an equivalent hydrophobic group contributed ~10-fold to antiviral potency. The positive charge on the HP would be expected to encourage negative charge on ligands, but we have consistently observed that negative charge on D is unfavorable. It is possible that ring D may not be specific for pocket binding interactions but instead may associate with lipid or other hydrophobic entity. Hydrophobicity, in addition to being a requirement to interact effectively with certain residues in the pocket, may encourage partitioning in areas near membrane where the HP is located.

*A polar substitution improved drug-likeness* Introducing a carbonyl or sulfonyl linker between C and D improved drug-like characteristics of the ligands without reducing potency. 10a, containing a sulfonyl linker, had the same activity (0.9 μM) as 9 m, containing a methylene linker, while logP was reduced by 2.7 units. The same 0.8–1.0 μM activity was observed for 10b (D = Boc), which contained a carbonyl in the linker and an −O-tBu group instead of substituted phenyl. This compound had logP reduced by 2 units and significantly lower molecular weight compared to 9 m. In docking studies, the carboxylate group on ring A of all compounds participated in a hydrogen bond with the $\varepsilon NH_2$ of Lys 574, while the sulfonyl or carbonyl groups in 10a or 10b, respectively, participated in an additional hydrogen bond with Gln 575′.

## 4. Conclusions

In conclusion, this study of small molecule intervention in the hydrophobic pocket of gp41 has revealed that a bisindole core in the molecular scaffold together with substantial hydrophobic character, logP ~7 or higher, was a necessary requirement for sub-μM inhibitory activity against HIV-1 fusion. Further enhancement of hydrophobicity was insufficient as a means of improving potency beyond a mid-nM level. Instead, potency could be promoted by adding specific polar interactions, taking into account a nearby Gln residue in predicted docked structures. SAR data suggested that the most effective molecules could also interact with lipids. The best compound to emerge from this study is 10b with logP = 6.8 and anti-fusion activity 0.8–1.0 μM. Hydrogen bonding between the Boc carbonyl group and pocket Gln 575′ may underlie its improved activity compared to other 3-ring compounds, providing the potential for improved specificity and drug-likeness. The compound has a molecular weight of 466.5da, on the small side for a PPI (typically ranging from 241 to 974 da [21]), leaving sufficient compound space for its optimization. While logP is still high, many optimization examples have shown that reduction in logP is possible using medicinal chemistry efforts [22].

## 5. Experimental section

### 5.1. Chemistry

The organic synthesis is described in Schemes 1 – 4 . Details of the syntheses are provided in the Supplementary Data. Intermediates 5a-e and 6a-n were obtained either from a commercial source or prepared according to Scheme S1 in the Supplementary Data. Scheme 1 shows the synthesis of bisindole compounds 9a-n. 9a, 9b and 9n are previously prepared compounds 1, 2 and 3, respectively (Fig. 1). 9o-q are corresponding fluorinated derivatives of 9n, prepared by the same method with available starting materials. 9◦ has trifluoromethoxy on ring D, 9p has both trifluoromethoxy on ring D and *m*-fluoro on ring A, 9q has 5-fluoro on ring B. 9r was prepared from 8a and 1-Boc-4-bromomethylpiperidine, and 9s was prepared according to Scheme 1 using 5d (3-methyl-6-bromoindole) and 6n as starting materials. Similarly 10a and 10b were prepared from 8a using the appropriate chemical group in place of 6.

Scheme 2 describes the synthesis of 3-ring systems 11b-e, including compounds substituted with an indazole or indoline in place of indole. For indazole compounds, reactions resulted in a mixture of 1 and 2-linked isomers, which were separated using flash chromatography and identified by COSY NMR. 11c1 (shown in Scheme 2B) and 11c2 are N1-methyl and N2-methyl isomers at ring C. Similar reactions to those shown were used to obtain different combinations of the ring systems. Scheme 2A was employed to make 11a using 5a and 6a as starting materials [2], 11f using 5c and 6a, and 11h using 5a and 6d. 11i was made as in Scheme 2B using 5-fluoro-6-bromoindole in place of 5b. 11g was made as in Scheme 2C using 5d in place of 5c.

Scheme 3 describes synthesis of 4-ring compounds 15b and 15c

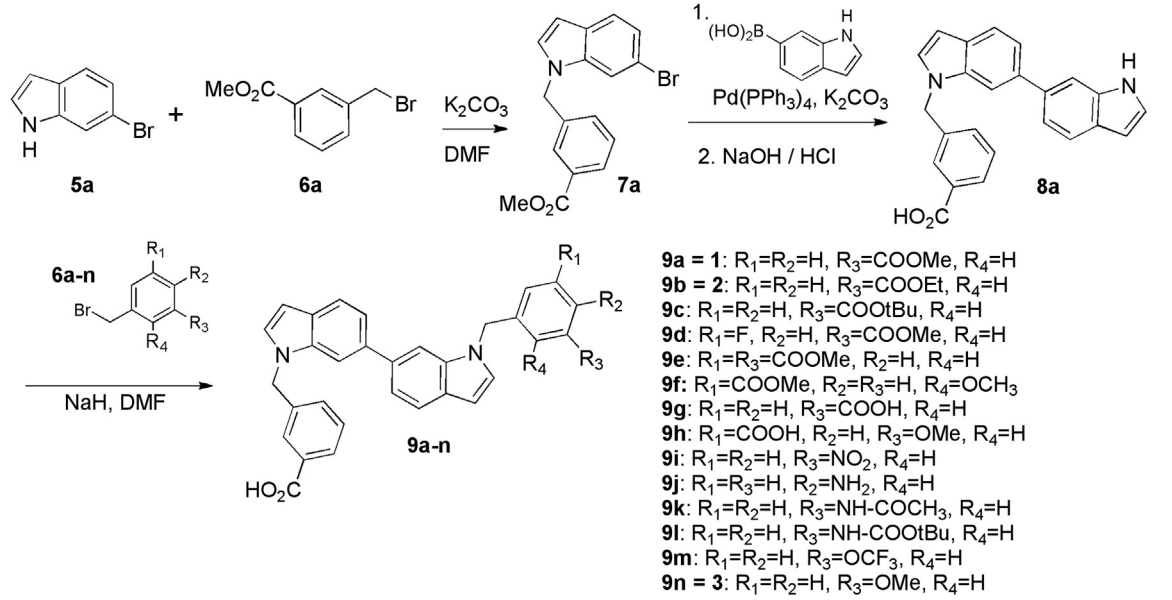


**Scheme 1.** Synthesis of 4-ring compounds **9a**-**9n**.

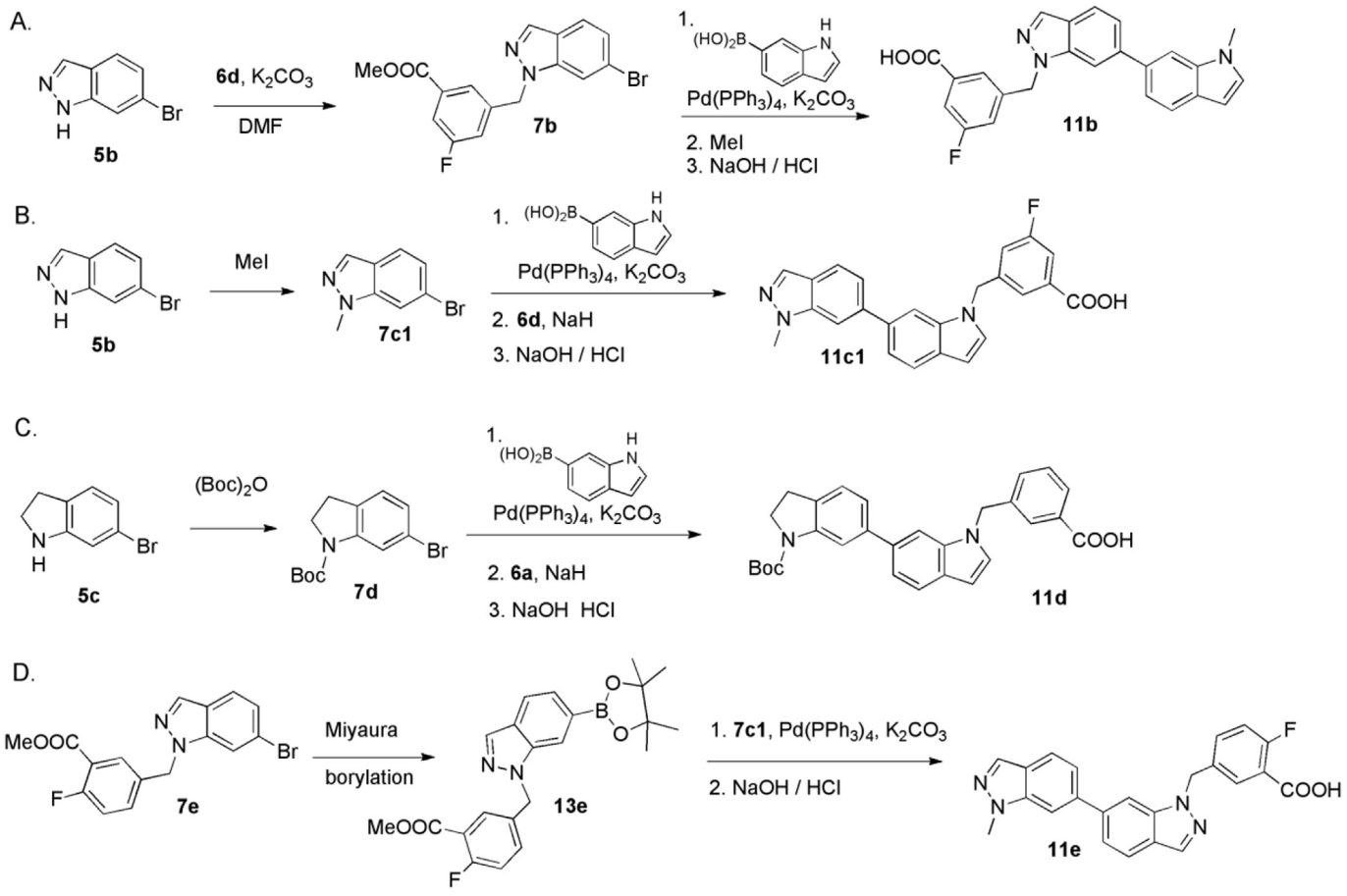


**Scheme 2.** Synthesis of 3-ring compounds **11b**-**11e**.

with one indole and one alternative fused ring structure. It also shows an improved method for the synthesis of 9a. Based on our practical experience, it was difficult to separate 9a from 8a by column chromatography, and the ester of 6a was labile in strong basic conditions. By employing a benzyl group to protect the carboxylic acid on 6-bromoindol-1-ylmethylbenzoic acid, followed by borylation and Suzuki coupling with 7a, we successfully obtained higher yield and easy purification of 9a. 15d is a fluorinated

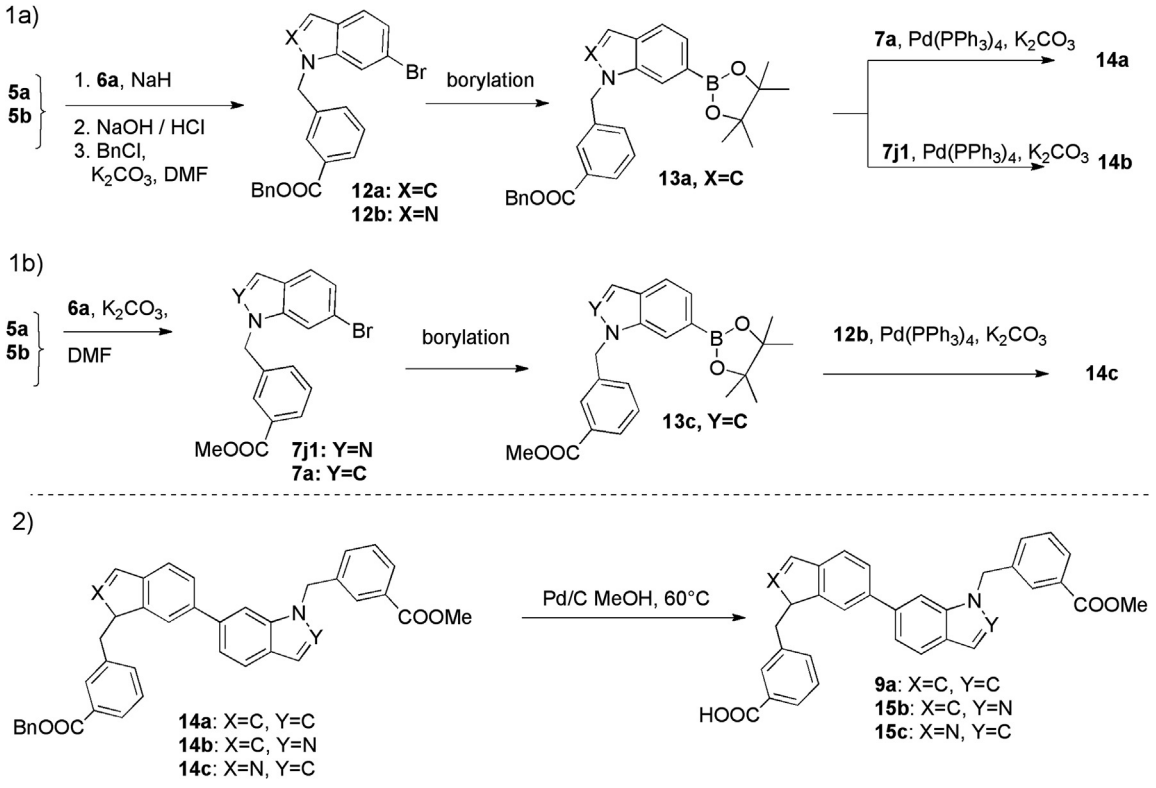


**Scheme 3.** Synthesis of 4-ring compounds containing a fused ring other than indole.

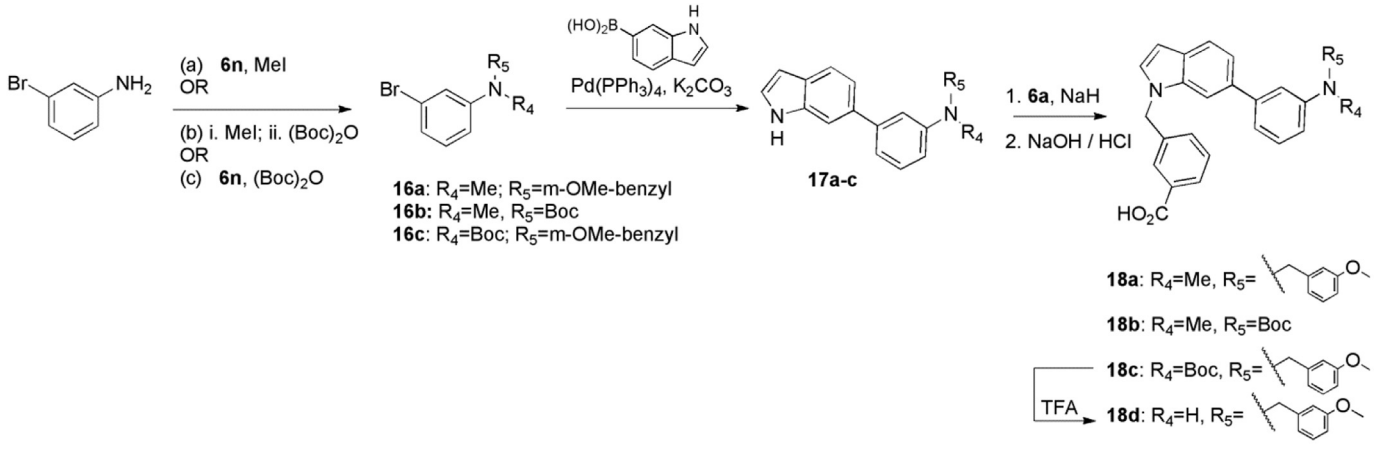


**Scheme 4.** Synthesis of aniline containing compounds.

derivative of 9a prepared by the same method. 15e was prepared using Scheme 2C but replacing the first Boc protection step with reaction of 5c with 6n. 15f, prepared using a procedure similar to Scheme 2A, contains an N2-substituted indazole at ring B.

Scheme 4 describes synthesis of aniline containing compounds 18a-d.

### 5.2. Compound properties

Compound properties are reported in Tables 1–4. Structures were optimized using LigPrep (LigPrep, Schrodinger, LLC, New York, NY, 2018). Pharmaceutically relevant properties including logP (water/octanol partition coefficient) and logS (aqueous solubility) were calculated using QikProp (QikProp, Schrodinger, LLC, New York, NY, 2018). Inhibition constants for HP-binding ($K_I$) were measured in a competitive inhibition fluorescence experiment [23] by concentration-dependent displacement of fluorescently labeled HP-binding C-peptide from the NHR binding site. Concentrations that yielded 50% inhibition of biological activity ($IC_{50}$) were obtained using cell-cell fusion ($IC_{50}^{CCF}$) and viral infectivity (virus-cell fusion; $IC_{50}^{VCF}$) assays as previously described [2]. Antiviral assays were run using lab-adapted viral strains Ba-L and IIIB. Details are in the Supplementary Data.

## Acknowledgements

This work was supported by National Institutes of Health (NIH) Grant AI122847 to MG and internal funds from Southern Research

Institute. Molecular graphics were produced using the Maestro program, provided free to academic users. We thank Schrodinger LLC, NY, NY for a free trial version of the ligand preparation and docking software.

## Appendix A. Supplementary data

Supplementary data to this article can be found online at https://doi.org/10.1016/j.ejmech.2018.10.048.

## References

[1] M. Gochin, G. Zhou, Amphipathic properties of HIV-1 gp41 fusion inhibitors, Curr. Top. Med. Chem. 11 (2011) 3022–3032.
[2] G. Zhou, V. Sofiyev, H. Kaur, B.A. Snyder, M.K. Mankowski, P.A. Hogan, R.G. Ptak, M. Gochin, Structure-activity relationship studies of indole-based compounds as small molecule HIV-1 fusion inhibitors targeting glycoprotein 41, J. Med. Chem. 57 (2014) 5270–5281.
[3] L. Lu, F. Yu, L. Cai, A.K. Debnath, S. Jiang, Development of small-molecule HIV entry inhibitors specifically targeting gp120 or gp41, Curr. Top. Med. Chem. 16 (2016) 1074–1090.
[4] L. Cai, S. Jiang, Development of peptide and small-molecule HIV-1 fusion inhibitors that target gp41, ChemMedChem 5 (2010) 1813–1824.
[5] D.C. Chan, C.T. Chutkowski, P.S. Kim, Evidence that a prominent cavity in the coiled coil of HIV type 1 gp41 is an attractive drug target, Proc. Natl. Acad. Sci. U.S.A. 95 (1998) 15613–15617.
[6] G. Zhou, D. Wu, B. Snyder, R.G. Ptak, H. Kaur, M. Gochin, Development of indole compounds as small molecule inhibitors of HIV-1 gp41, J. Med. Chem. 54 (2011) 7220–7231.
[7] F. Naider, J. Anglister, Peptides in the treatment of AIDS, Curr. Opin. Struct. Biol. 19 (2009) 473–482.
[8] Y. He, S. Liu, W. Jing, H. Lu, D. Cai, D.J. Chin, A.K. Debnath, F. Kirchhoff, S. Jiang, Conserved residue Lys574 in the cavity of HIV-1 Gp41 coiled-coil domain is critical for six-helix bundle stability and virus entry, J. Biol. Chem. 282 (2007) 25631–25639.
[9] X. Ran, J.E. Gestwicki, Inhibitors of protein-protein interactions (PPIs): an analysis of scaffold choices and buried surface area, Curr. Opin. Chem. Biol. 44 (2018) 75–86.
[10] J.A. Wells, C.L. McClendon, Reaching for high-hanging fruit in drug discovery at protein-protein interfaces, Nature 450 (2007) 1001–1009.
[11] M.A. Kuenemann, L.M. Bourbon, C.M. Labbe, B.O. Villoutreix, O. Sperandio, Which three-dimensional characteristics make efficient inhibitors of protein-protein interactions? J. Chem. Inf. Model. 54 (2014) 3067–3079.
[12] G. Fischer, M. Rossmann, M. Hyvonen, Alternative modulation of protein-protein interactions by small molecules, Curr. Opin. Biotechnol. 35 (2015) 78–85.
[13] G. Zhou, D. Wu, E. Hermel, E. Balogh, M. Gochin, Design, synthesis, and evaluation of indole compounds as novel inhibitors targeting Gp41, Bioorg. Med. Chem. Lett 20 (2010) 1500–1503.
[14] B. Strockbine, R.C. Rizzo, Binding of antifusion peptides with HIVgp41 from molecular dynamics simulations: quantitative correlation with experiment, Proteins 67 (2007) 630–642.
[15] H.J. Bohm, D. Banner, S. Bendels, M. Kansy, B. Kuhn, K. Muller, U. Obst-Sander, M. Stahl, Fluorine in medicinal chemistry, Chembiochem 5 (2004) 637–643.
[16] E.P. Gillis, K.J. Eastman, M.D. Hill, D.J. Donnelly, N.A. Meanwell, Applications of fluorine in medicinal chemistry, J. Med. Chem. 58 (2015) 8315–8359.
[17] D.D. Gaikwad, A.D. Chapolikar, C.G. Devkate, K.D. Warad, A.P. Tayade, R.P. Pawar, A.J. Domb, Synthesis of indazole motifs and their medicinal importance: an overview, Eur. J. Med. Chem. 90 (2015) 707–731.
[18] J. Hu, Y. Wang, Y. Li, D. Cao, L. Xu, S. Song, M.S. Damaneh, J. Li, Y. Chen, X. Wang, L. Chen, J. Shen, Z. Miao, B. Xiong, Structure-based optimization of a series of selective BET inhibitors containing aniline or indoline groups, Eur. J. Med. Chem. 150 (2018) 156–175.
[19] A. Aguilar, J. Lu, L. Liu, D. Du, D. Bernard, D. McEachern, S. Przybranowski, X. Li, R. Luo, B. Wen, D. Sun, H. Wang, J. Wen, G. Wang, Y. Zhai, M. Guo, D. Yang, S. Wang, Discovery of 4-((3'R,4'S,5'R)-6''-Chloro-4'-(3-chloro-2-fluorophenyl)-1'-ethyl-2''-oxodispiro[ cyclohexane-1,2'-pyrrolidine-3',3''-indoline]-5'-carboxamido)bicyclo[2.2.2]octane -1-carboxylic acid (AA-115/APG-115): a potent and orally active murine double minute 2 (MDM2) inhibitor in clinical development, J. Med. Chem. 60 (2017) 2819–2839.
[20] P.D. Leeson, B. Springthorpe, The influence of drug-like concepts on decision-making in medicinal chemistry, Nat. Rev. Drug Discov. 6 (2007) 881–890.
[21] A.P. Higueruelo, A. Schreyer, G.R. Bickerton, W.R. Pitt, C.R. Groom, T.L. Blundell, Atomic interactions and profile of small molecules disrupting protein-protein interfaces: the TIMBAL database, Chem. Biol. Drug Des. 74 (2009) 457–467.
[22] A.L. Hopkins, G.M. Keseru, P.D. Leeson, D.C. Rees, C.H. Reynolds, The role of ligand efficiency metrics in drug discovery, Nat. Rev. Drug Discov. 13 (2014) 105–121.
[23] L. Cai, M. Gochin, A novel fluorescence intensity screening assay identifies new low molecular weight inhibitors of the gp41 coiled coil domain of HIV-1, Antimicrob. Agents Chemother. 51 (2007) 2388–2395.